Elastic and thermal properties of some ternary β-Ti based alloys

Sergey O. Kasparyan[1,2,a], Adil E. Ordabaev[2,b], Alexander V. Bakulin[1,c], Svetlana E. Kulkova[1,d]

[1]Institute of Strength Physics and Materials Science of the Siberian Branch of the Russian Academy of Sciences, Tomsk, Russia

[2]National Research Tomsk State University, Tomsk, Russia

[a]ks-ftf-isopams@mail.ru, [b]adil.ordabaev04@gmail.com, [c]bakulin@ispms.ru, [d]kulkova@ispms.ru

Corresponding author: Sergey O. Kasparyan, ks-ftf-isopams@mail.ru

ABSTRACT The elastic moduli and some thermal properties of four series of ternary β-Ti based alloys of the XY_3Ti_{11} composition, where X and Y are elements of IVB–VIB, IIIA and IVA groups, have been studied using the projector augmented wave method within the density functional theory. It has been shown that the calculated Young's moduli in these series of alloys are lower than those in commercially pure α-Ti titanium or in the Ti-6Al-4V alloy. With an increase in the concentration of s, p-elements and the number of electrons in the d-band of the X-metal, the Young's modulus tends to decrease. The variation of Debye temperature, acoustic Grüneisen parameter and thermal conductivity in titanium alloy series is discussed. It is shown that high thermal conductivity correlates with high Debye temperature, which in turn increases with increase of the values of the Young's modulus.

1. Introduction

Due to the combination of biocompatibility and unique mechanical properties, such as shape memory effect and the ability to achieve a low Young's modulus (E), β-Ti based alloys are considered promising for use in medicine [1–3]. Currently, the most commonly used material for orthopedic and dental implants is commercially pure (CP) titanium or an alloy of the composition Ti-6Al-4V [3–6]. At the same time, titanium remains a universal structural material and is widely used in the aerospace, automotive, and shipbuilding industries, in particular, for aircraft skins, various fasteners, chassis parts, rocket engines, etc. Due to its high strength and heat resistance, titanium and its alloys can withstand significant loads. Since titanium does not react with salt water, materials based on it are widely used in shipbuilding. In addition, titanium demonstrates excellent corrosion resistance. This property explains the popularity titanium has gained in the chemical process and power generation industry where harsh environments are usual. It is used to manufacture key equipment for the chemical and petrochemical industries. However, the addition of alloying impurities can significantly affect its mechanical and physicochemical properties.

It is known that the addition of bioinert β-stabilizing elements such as Mo, Nb, Ta, etc. extends the temperature range of β-Ti stability [7], and the addition of Zr and some s, p-elements (e.g. Sn, In) leads to a decrease in Young's modulus. Recently, a "cluster plus glue atom" model [8] was proposed to search for new low-modulus ternary titanium alloys, where the alloying atom (X) is located in the center of the titanium cluster, with 8 atoms on the first and 6 atoms on the second coordination sphere, and additional element (Y) plays the role of "glue atom". It is believed that they should weakly interact with the Ti atoms. Within this model, a theoretical study of the elastic moduli of a number of ternary titanium alloys was carried out [9], and three types of clusters with the number of Y atoms equal to 1, 3 and 4 were considered. The authors showed that in the case of $TaNb_3Ti_{11}$, the Young's modulus exhibits the lowest value of ~ 7 GPa. In work [10], calculations of the electronic structure and elastic properties of a number of ordered XY_3Ti_{11} alloys were also carried out using the model [8] and it was found that all the alloys considered have Young's modulus values lower than CP titanium, and for five alloys it is even lower than 45 GPa. However, in both works [9, 10], only transition metals were used as X and Y elements.

The aim of this work is to study the elastic moduli of four series of titanium alloys of the XY_3Ti_{11} composition with In and Sn both at the X and Y positions, which will allow us to identify their role in reducing the Young's modulus. Besides such series of ternary Ti-based alloys are very convenient models for study not only elastic properties but also

for calculation of thermal properties, which are less studied by DFT methods [11, 12]. Thus, we calculate the Debye temperature, acoustic Grüneisen parameter and thermal conductivity of the alloys and reveal their trends in dependence on the alloy composition.

2. Computational details

The electronic structure and elastic properties of ternary titanium alloys were calculated using the projector augmented wave method [13, 14] within the VASP code [15, 16] with a generalized gradient approximation for the exchange-correlation functional in the form of PBE–GGA [17]. The maximum energy of plane waves from the basis set was 300 eV. Integration over the Brillouin zone was performed using a $12 \times 12 \times 12$ Monkhorst–Pack k-point grid [18]. Full optimization of the atomic structure of the alloys included both the relaxation of atomic positions and a change in the cell volume. Convergence was considered achieved if the difference in the total energies of two successive iterations did not exceed 10^{-6} eV. The convergence criterion for the forces acting on the atoms was 10^{-3} eV/Å.

The elastic constants were estimated using the finite difference method, based on the analysis of the change in the total energy of the system during deformation. The bulk modulus was calculated using the following formula:

$$B = (C_{11} + 2C_{12})/3. \tag{1}$$

To estimate the stability of the alloys, the Born criteria [19] $C_{44} > 0$, $C_{11} - C_{12} = 2C' > 0$, and $C_{11} + 2C_{12} > 0$ were used. The shear moduli (G) and Young's moduli (E), as well as Poisson's ratio (ν) were calculated within the Voigt–Reuss–Hill model [20], which averages the values of elastic moduli calculated using the Voigt (V) [21] and Reuss (R) [22] methods:

$$G = \frac{G_V + G_R}{2}, \quad E = \frac{9BG}{3B + G}, \quad v = \frac{3B - 2G}{2(3B + G)}, \tag{2}$$

$$G_V = \frac{C_{11} - C_{12} + 3C_{44}}{5}, \quad G_R = \frac{5(C_{11} - C_{12})C_{44}}{4C_{44} + 3(C_{11} - C_{12})}. \tag{3}$$

Note that for cubic systems $B = B_V = B_R$.

3. Results and discussion

3.1. Elastic properties

Tables 1 and 2 present the calculated elastic constants and moduli for the studied series of alloys. All considered alloys in accordance with above-mentioned Born criteria [19] are stable. However, the minimum values of C' are observed in the following systems: InHf$_3$Ti$_{11}$ (first series), SnHf$_3$Ti$_{11}$ (second series), CrIn$_3$Ti$_{11}$ (third series), and WSn$_3$Ti$_{11}$ (fourth series), which indicates their proximity to the critical threshold of mechanical stability. It is seen that the constant C_{11}, which characterizes the interaction between the elements X and Y with the titanium atoms in the second coordination spheres, demonstrates a tendency to increase with the number of electrons in the d-band of the transition element. In the studied systems the values of the constant C_{44} are significantly lower than the other elastic constants, which causes a positive value of the difference $(C_{11} - C_{44})$, known as the Cauchy pressure. A positive value of this parameter is traditionally associated with the metallic bond.

Comparison of the systems with Sn and In at the X-position revealed a slight increase in the C_{11} and C_{12} values in Sn-containing alloys, while C_{44} demonstrates a weakly expressed growth in In-containing alloys. The lowest C' values are in the alloys with Zr and Hf, which is consistent with the previously noted trend. In the systems with In and Sn at the Y-position, a correlation was observed between the changes in the C' and C_{44} constants, with the latter having values significantly higher than in the alloys of the first two series. In general, the C_{11} constants are lower in the last two series, which indicates a decrease in the interatomic interaction in these alloys with an increase in the concentration of s, p-elements.

The results of elastic moduli calculations demonstrate the following trend: $B > E > G$ is observed for almost all alloy series (Fig. 1). The shear modulus is characterized by comparatively low values. The lowest values of Young's modulus in each series were: 37.3 GPa for InHf$_3$Ti$_{11}$, 36.5 GPa for SnHf$_3$Ti$_{11}$, 65.7 GPa for CrIn$_3$Ti$_{11}$ and 52.4 GPa for WSn$_3$Ti$_{11}$ (Fig. 1). At the same time, low values of Young's modulus correspond to low values of elastic constant C_{11} (shown by bold in Tables 1 and 2). It should be noted that the values of Young's modulus for the studied alloys are lower than for pure titanium and Ti-6Al-4V alloy ($105 - 120$ GPa [23, 24]). However, these results were obtained for α-phase. Of particular interest are InHf$_3$Ti$_{11}$ and SnHf$_3$Ti$_{11}$ alloys, demonstrating the lowest values of Young's modulus, which makes them promising for further research in the context of biomedical application. In addition, a relationship was found between the increase in the number of valence d-electrons and the growth of the bulk modulus B in the In(Sn)Y$_3$Ti$_{11}$ alloy series. In general, the alloys with In and Sn elements at the X-position exhibit close values of all moduli (Table 1). Young's modulus in the series of alloys with In and Sn at the Y-position (Table 2) demonstrates a tendency to decrease in value with an increase in the number of electrons in the d-band of the X-element. High values of Young's modulus in the series of alloys with Sn correlate with high values of the shear modulus in the case of Zr and Hf.
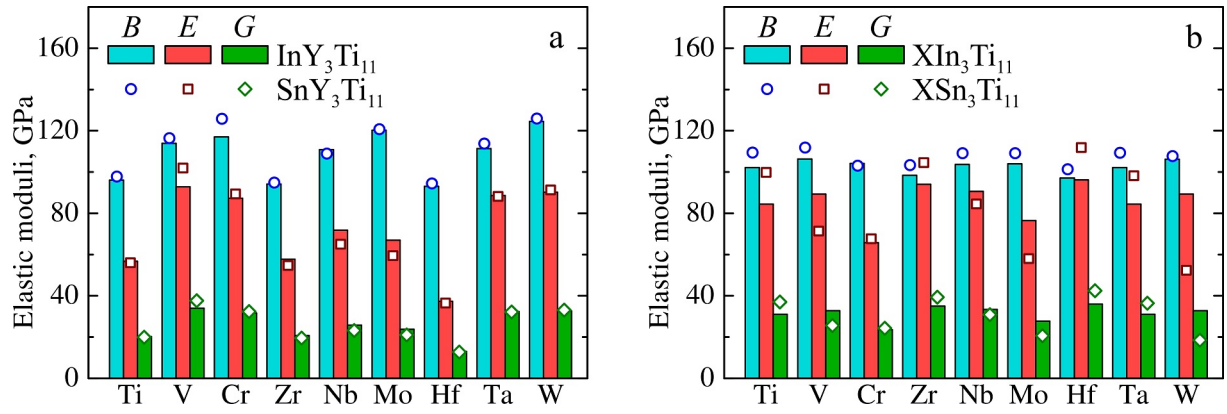
FIG. 1. Theoretical elastic moduli in dependence on the number of valence d-electrons in alloys In(Sn)Y$_3$Ti$_{11}$ (a) and XIn(Sn)$_3$Ti$_{11}$ (b) with metals of IVB–VIB groups

TABLE 1. Elastic constant and moduli (in GPa) for series of alloys InY$_3$Ti$_{11}$ and SnY$_3$Ti$_{11}$

Alloy	C_{11}	C_{12}	C_{44}	B	G	E	Alloy	C_{11}	C_{12}	C_{44}	B	G	E
InTi$_3$Ti$_{11}$	110.5	88.8	30.7	96.1	20.2	56.7	SnTi$_3$Ti$_{11}$	111.1	91.2	31.6	97.8	19.9	56.0
InV$_3$Ti$_{11}$	157.7	92.1	34.8	113.9	34.0	92.8	SnV$_3$Ti$_{11}$	164.4	92.5	38.8	116.4	37.6	101.9
InCr$_3$Ti$_{11}$	174.0	88.5	25.9	117.0	31.7	87.3	SnCr$_3$Ti$_{11}$	185.9	95.8	25.9	125.8	32.4	89.4
InZr$_3$Ti$_{11}$	109.0	86.7	31.2	94.1	20.7	57.7	SnZr$_3$Ti$_{11}$	109.8	87.5	28.3	94.9	19.5	54.7
InNb$_3$Ti$_{11}$	140.5	96.0	28.4	110.8	25.8	71.8	SnNb$_3$Ti$_{11}$	135.7	95.5	25.6	108.9	23.2	65.0
InMo$_3$Ti$_{11}$	155.7	102.4	22.0	120.2	23.8	66.9	SnMo$_3$Ti$_{11}$	148.7	106.6	21.0	120.7	21.0	59.5
InHf$_3$Ti$_{11}$	**96.3**	91.3	32.5	93.0	13.0	**37.3**	SnHf$_3$Ti$_{11}$	**97.8**	92.9	31.6	94.5	12.7	**36.5**
InTa$_3$Ti$_{11}$	140.5	96.6	42.1	111.3	32.4	88.6	SnTa$_3$Ti$_{11}$	142.5	99.4	42.1	113.8	32.2	88.2
InW$_3$Ti$_{11}$	163.7	104.9	35.1	124.5	32.7	90.2	SnW$_3$Ti$_{11}$	163.6	107.0	36.8	125.9	33.1	91.3

TABLE 2. Elastic constant and moduli (in GPa) for series of alloys XIn$_3$Ti$_{11}$ and XSn$_3$Ti$_{11}$

Alloy	C_{11}	C_{12}	C_{44}	B	G	E	Alloy	C_{11}	C_{12}	C_{44}	B	G	E
TiIn$_3$Ti$_{11}$	116.8	94.8	60.0	102.1	31.0	84.4	TiSn$_3$Ti$_{11}$	132.7	97.8	60.9	109.4	37.0	99.8
VIn$_3$Ti$_{11}$	121.4	98.7	64.4	106.3	32.8	89.3	VSn$_3$Ti$_{11}$	121.5	106.9	55.1	111.8	25.6	71.4
CrIn$_3$Ti$_{11}$	**113.1**	99.8	50.9	104.2	23.6	**65.7**	CrSn$_3$Ti$_{11}$	113.2	97.8	50.0	103.0	24.3	67.7
ZrIn$_3$Ti$_{11}$	119.4	87.9	59.3	98.4	35.0	94.0	ZrSn$_3$Ti$_{11}$	130.0	89.9	61.6	103.3	39.3	104.6
NbIn$_3$Ti$_{11}$	122.1	94.5	59.6	103.7	33.4	90.6	NbSn$_3$Ti$_{11}$	126.6	100.4	54.0	109.1	30.8	84.5
MoIn$_3$Ti$_{11}$	118.1	97.0	51.7	104.0	27.7	76.4	MoSn$_3$Ti$_{11}$	117.2	105.1	43.6	109.1	20.6	58.0
HfIn$_3$Ti$_{11}$	118.5	86.4	61.4	97.1	36.0	96.2	HfSn$_3$Ti$_{11}$	131.1	86.4	65.1	101.3	42.5	111.8
TaIn$_3$Ti$_{11}$	116.8	94.8	60.0	102.1	31.0	84.4	TaSn$_3$Ti$_{11}$	132.4	97.8	59.4	109.3	36.4	98.2
WIn$_3$Ti$_{11}$	121.4	98.7	64.4	106.2	32.8	89.3	WSn$_3$Ti$_{11}$	**111.6**	105.7	48.3	107.7	18.5	**52.4**

There are several approaches to estimate the ductile/brittle behavior of materials. In [25] the ratio of the shear modulus to the bulk modulus is used for these purposes: the values $G/B < 0.5$ correspond to ductile behavior, and $G/B > 0.5$ to brittle behavior. As can be seen from Fig. 2a, the G/B values for all series of alloys are below 0.5. The second approach [25] is that in ductile materials, the Poisson's ratio (ν) should be greater than 1/3. From Fig. 2b, it is seen that ν is generally greater than this value, with the exception of the HfSn$_3$Ti$_{11}$ alloy, while the ν values for HfIn$_3$Ti$_{11}$ and ZrSn$_3$Ti$_{11}$ correspond to the critical value. In addition, the values of Poisson's ratio are used to analyze the nature of the chemical bond in the systems. Thus, the value $\nu \approx 0.25$ indicates an ionic bond, which corresponds exactly to brittle fracture, while high values ν indicate a strong metallic bond and good toughness.
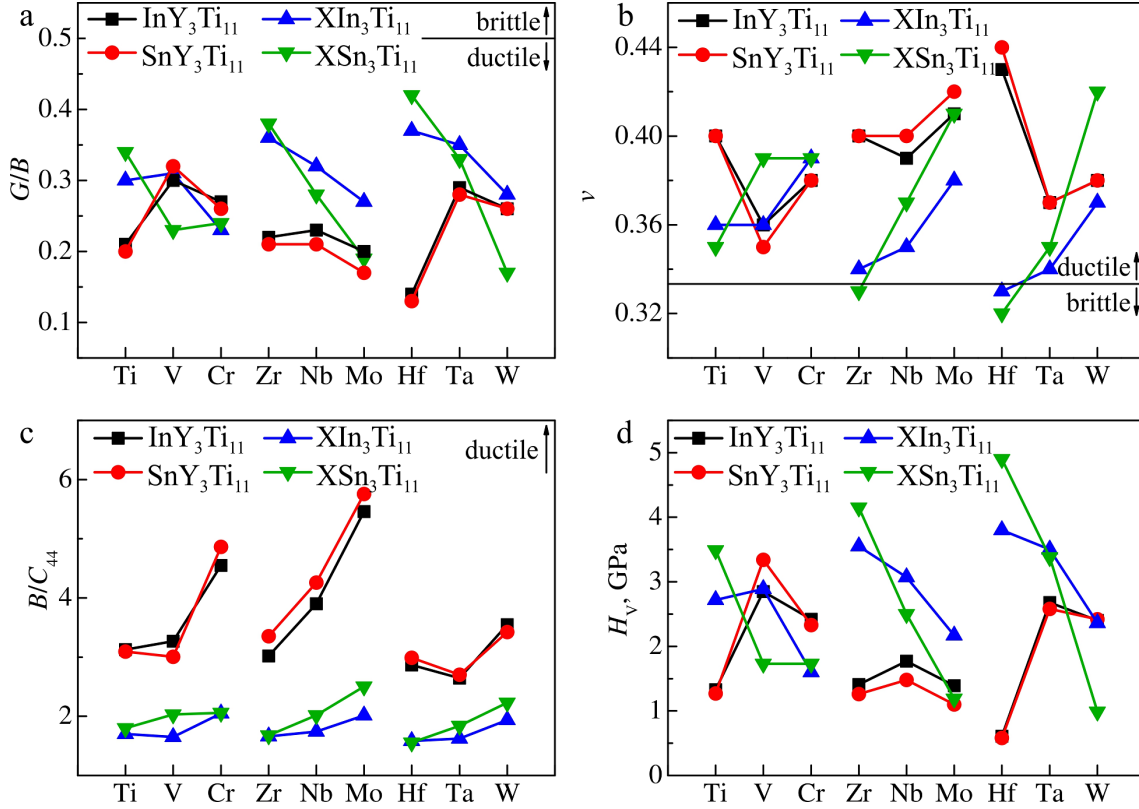

FIG. 2. Pugh's ratio G/B (a), Poisson's coefficient ν (b), B/C_{44} (c), and H_V for the alloys In(Sn)Y$_3$Ti$_{11}$ and XIn(Sn)$_3$Ti$_{11}$

In addition, an increase in the ratio of the bulk modulus to the C_{44} constant [25] can also correlate with a decrease in the brittleness of the material. It is seen from Fig. 2c that in general these values are greater than ~ 1.5, while the values for the InY$_3$Ti$_{11}$ and SnY$_3$Ti$_{11}$ alloy series are higher than for alloys with simple metals in the Y-position. The Vickers hardness of the alloys was also estimated using the following empirical relationship [26]:

$$H_V = 0.92 \, (G/B)^{1.137} \, G^{0.708}. \tag{4}$$

Vickers hardness is used to evaluate the ability of materials to resist deformation under compressive stress. Several empirical formulas were proposed for its calculation, as shown in our earlier work [27]. Fig. 2d demonstrates that the microhardness in XSn$_3$Ti$_{11}$ alloys with metals of IVB group is increased from 3.5 to 4.9 GPa in the set of isoelectronic elements. These values are significantly higher than that of 1.8 GPa for Ti-6Al-4V. High microhardness values are observed for In(Sn)Y$_3$Ti$_{11}$ alloys with V and XIn$_3$Ti$_{11}$ alloys with V, Nb, Ta (Table 3). In addition, other parameters that are also used to describe brittle/ductile behavior were also calculated, in particular, the fracture toughness (K_{IC}) and the brittleness index (M_{dt}). Fracture toughness characterizes the resistance to crack propagation, and the brittleness index reflects the damage resistance and can be determined using H_V and K_{IC} [28, 29], and the large value of the M_{dt} means a weak damage tolerance. The K_{IC} and M_{dt} were obtained from the following expressions:

$$K_{IC} = V_0^{1/6} G \left(\frac{B}{G} \right)^{1/2}, \tag{5}$$

$$M_{dt} = \frac{H_V}{K_{IC}}, \tag{6}$$

TABLE 3. Calculated values of Vickers microhardness H_V (in GPa), fracture toughness K_{IC} (in MPa·m$^{1/2}$), and brittleness index M_{dt} (in μm$^{-1/2}$)

Alloy	H_V	K_{IC}	M_{dt}	Alloys	H_V	K_{IC}	M_{dt}	Alloy	H_V	K_{IC}	M_{dt}
InTi$_3$Ti$_{11}$	1.33	0.71	1.87	SnTi$_3$Ti$_{11}$	1.27	0.71	1.78	TiIn$_3$Ti$_{11}$	2.72	0.92	2.97
InV$_3$Ti$_{11}$	**2.85**	1.00	**2.86**	SnV$_3$Ti$_{11}$	**3.34**	1.07	**3.12**	VIn$_3$Ti$_{11}$	2.89	0.96	3.01
InCr$_3$Ti$_{11}$	2.42	0.99	2.44	SnCr$_3$Ti$_{11}$	2.33	1.03	2.25	CrIn$_3$Ti$_{11}$	1.60	0.80	1.99
InZr$_3$Ti$_{11}$	1.41	0.72	1.96	SnZr$_3$Ti$_{11}$	1.26	1.10	1.14	ZrIn$_3$Ti$_{11}$	3.55	0.96	3.70
InNb$_3$Ti$_{11}$	1.77	0.87	2.04	SnNb$_3$Ti$_{11}$	1.48	1.28	1.16	NbIn$_3$Ti$_{11}$	3.07	0.96	3.20
InMo$_3$Ti$_{11}$	1.39	0.86	1.61	SnMo$_3$Ti$_{11}$	1.10	0.81	1.36	MoIn$_3$Ti$_{11}$	2.17	0.87	2.48
InHf$_3$Ti$_{11}$	0.61	0.57	1.08	SnHf$_3$Ti$_{11}$	0.58	0.56	1.03	HfIn$_3$Ti$_{11}$	**3.80**	0.97	**3.93**
InTa$_3$Ti$_{11}$	2.68	0.97	2.75	SnTa$_3$Ti$_{11}$	2.58	0.98	2.63	TaIn$_3$Ti$_{11}$	3.50	0.98	3.57
InW$_3$Ti$_{11}$	2.40	1.03	2.33	SnW$_3$Ti$_{11}$	2.42	1.05	2.32	WIn$_3$Ti$_{11}$	2.36	0.89	2.64

where V_0 is the cell volume per atom (in m^3). The obtained values of these parameters are given in Table 3.

It is seen from Table 3 that for alloys with In and Sn in the X-position the scatter in the K_{IC} parameter depending on the transition metal (Y) is larger (0.56 – 1.28 MPa·m$^{1/2}$) than that in the series of alloys with simple elements in the Y-position (0.72 – 1.04 MPa·m$^{1/2}$), and the influence of Sn on this scatter is more significant than that of In. The values of the K_{IC} parameter in the considered series of alloys are significantly lower than the values obtained for c-CrH (3.42 MPa·m$^{1/2}$ [11]), AlN (2.79 MPa·m$^{1/2}$ [30]), c-BN (5 MPa·m$^{1/2}$ [30]) or for V(Nb)$_5$Si$_3$B compounds ($\sim$4.0 – 4.70 MPa·m$^{1/2}$ [12]). At the same time, the values of the brittleness index for the studied alloys are significantly lower than for the compounds indicated above. In the series with In and Sn in the X-position, the lowest M_{dt} value corresponds to alloys with Hf, and the highest – to those with V (Table 3). With increasing concentration of simple metals, the brittleness index increases, and the maximum values of 3.93 and 4.58 μm$^{-1/2}$ were obtained for alloys with Hf in the X-position. That is, a decrease in the hafnium concentration leads to a decrease in the damage resistance of the alloys.

3.2. Thermal properties

It is known that the free energy is significantly affected by lattice vibrations, which can be characterized in terms of the Debye temperature Θ_D and the Grüneisen constant γ_a [31]. In addition, the bond strength between atoms can also correlate with the Debye temperature: a strong bond strength corresponds to a high Debye temperature [32]. The Debye temperature of alloys can be calculated using the formula from [33]:

$$\Theta_D = \frac{h}{k_B} \left[\frac{3n}{4\pi} \left(\frac{N_A \rho}{M} \right) \right]^{1/3} v_m, \tag{7}$$

where h and k_B are the Planck and Boltzmann constants, N_A is the Avogadro constant, n is the number of atoms in the alloy, ρ is the density of the substance, M is its molecular weight, v_m is the average sound velocity, which can be calculated using the following formula from [34]:

$$v_m = \left[\frac{1}{3} \left(\frac{2}{v_t^3} + \frac{1}{v_l^3} \right) \right]^{-1/3}, \tag{8}$$

where v_t and v_l are the transverse and longitudinal sound velocities, respectively, which are obtained from the following expressions:

$$v_l = \left(\frac{B + 4G/3}{\rho} \right)^{1/2}, \tag{9}$$

$$v_t = \left(\frac{G}{\rho} \right)^{1/2}. \tag{10}$$

It is known that in order to study the thermal expansion or thermal conductivity of crystals, it is necessary to use a nonharmonic approximation to describe the interaction of atoms. For these purposes, it is necessary to know the acoustic Grüneisen parameter γ_a, which was calculated as in [35]:

$$\gamma_a = \frac{3}{2} \left(\frac{3v_l^2 - 4v_t^2}{v_l^2 + 2v_t^2} \right). \tag{11}$$

Table 4 presents the values of the density (ρ) of the alloys, which was estimated as the mass of atoms in the computational cell divided by its volume, the sound velocities (longitudinal v_l, transverse v_t and average v_m), the acoustic Grüneisen parameter γ_a, and the Debye temperature Θ_D for two series of alloys with In at the X and Y positions that is with increase of In concentration. Since there are no corresponding experimental data on the Debye temperature for the studied alloys, we estimated it for the Ti-6Al-4V alloy (Ti-10.2Al-3.6V at. %) in the β phase, while the elastic constants were calculated using the EMTO-CPA method [36], which takes into account the disordering effect. The obtained value of Θ_D according to formula (7) is 315.6 K, which agrees well with the experimental value of 326.0 K [37]. The values of Θ_D in dependence on elastic anisotropy are 264.2 – 278.2 K [23]. The estimation for β-Ti in the used model with a vacancy (i.e. Ti also occupies X and Y positions in the computational cell) gives the value 251.8 K that is smaller in comparison with the previous cases. That is, the decrease of the Debye temperature means a decrease in the bond strength and a lower hardness. The smallest Θ_D in alloy with Hf in the Y-position (Table 4), indicating the lowering of bond strength, that correlates with the lowest Young's modulus (Table 1) and hardness (Fig. 2d) as well as with the largest γ_a. In the case of alloy with Hf in the X-position, an increase in Θ_D and, consequently, the bond strength and H_V is observed. It should be noted that a correlation between the Debye temperature and Young's modulus takes place for all studied series of alloys. The obtained Debye temperatures of the alloys are subsequently used to calculate their lattice thermal conductivity.

TABLE 4. Density ρ (in g/cm^3), sound velocities (longitudinal v_l, transverse v_t and average v_m in m/s), acoustic Grüneisen parameter γ_a, and Debye temperature Θ_D (in K)

Alloy	ρ	v_l	v_t	v_m	γ_a	Θ_D	Alloy	ρ	v_l	v_t	v_m	γ_a	Θ_D
InTi$_3$Ti$_{11}$	4.877	5023	2037	2306	2.64	263.2	TiIn$_3$Ti$_{11}$	5.458	5125	2382	2682	2.24	301.6
InV$_3$Ti$_{11}$	5.176	5547	2563	2888	**2.26**	**334.8**	VIn$_3$Ti$_{11}$	5.545	5201	2433	2739	2.22	309.2
InCr$_3$Ti$_{11}$	5.379	5512	2448	2762	2.38	324.0	CrIn$_3$Ti$_{11}$	5.580	4929	2054	2324	2.57	262.8
InZr$_3$Ti$_{11}$	5.332	4777	1968	2227	2.60	248.8	ZrIn$_3$Ti$_{11}$	5.608	5086	2499	2806	2.06	**313.5**
InNb$_3$Ti$_{11}$	5.621	5082	2141	2421	2.53	274.8	NbIn$_3$Ti$_{11}$	5.707	5097	2420	2722	2.17	305.8
InMo$_3$Ti$_{11}$	5.905	5070	2006	2273	2.71	261.3	MoIn$_3$Ti$_{11}$	5.778	4939	2190	2472	2.38	278.5
InHf$_3$Ti$_{11}$	6.900	3999	1373	1561	**3.07**	**174.8**	HfIn$_3$Ti$_{11}$	6.138	4861	2422	2718	2.01	304.0
InTa$_3$Ti$_{11}$	7.207	4629	2120	2389	2.28	270.8	TaIn$_3$Ti$_{11}$	6.241	4894	2387	2682	2.08	301.4
InW$_3$Ti$_{11}$	7.511	4730	2086	2355	2.40	269.9	WIn$_3$Ti$_{11}$	6.316	4756	2144	2418	2.33	272.6

It is known that the acoustic Grüneisen parameter γ_a is related to scattering between phonons. The larger γ_a means the more inharmonic the phonons behavior, which in turn leads to lower thermal conductivity. The values of γ_a were calculated using formula (11) and the Leontiev formula [38], which used not only the average value of the sound velocities, but also density of material and bulk modulus. In the case of the test alloy Ti-6Al-4V, almost the same values of γ_a equal ~ 2.50 were obtained. However, the experimental value from paper [37] is more than two times smaller (1.100), since the so-called thermodynamic Grüneisen parameter is usually measured in experiment. As noted earlier in [39], the acoustic Grüneisen parameter can differ significantly from the thermodynamic parameter (γ_D), for example, for rare earth elements the difference in these coefficients reaches an average of two times. Our calculation of the acoustic Grüneisen parameters for Nb, Ta and other metals shows a similar trend. It is seen from Table 4 that an increase in γ_a in the InY$_3$Ti$_{11}$ alloy series is observed in the case of 4d-metals, as well as Ti and Hf in the Y-position. In the case of Sn in the Y-position, large γ_a values are characteristic of VIB metals.

A few words should be added about the sound velocities which are used for calculation of both characteristics Θ_D and γ_a. It is well known that the sound velocities in crystal with cubic symmetry are determined by elastic constants (Table 1) or their combinations depending on the direction of propagation. Since standard formulas for calculating the longitudinal and transverse sound velocities (Table 5) were used [40], they are not given. The longitudinal sound velocity along the [100] direction is related to the elastic constant C_{11}, which increases with the number of d-electrons of the transition metals, therefore we observe an increase in the [100]v_l in the series InTi$_3$Ti$_{11}$–InV$_3$Ti$_{11}$–InCr$_3$Ti$_{11}$ (Table 5) and in the case of metals isoelectronic to the Y-element. The transverse two modes are related to elastic constant C_{44}, which is significantly lower than C_{11}, therefore the values of v_{t1} and v_{t2} are equal and almost two times smaller than the value of the v_l. In the case of the [110] direction, the value of v_l is the highest, and the transverse velocities are different in accordance with their determination. Finally, in the case of the [111] direction, the longitudinal sound velocity reaches a maximum for VB elements for InY$_3$Ti$_{11}$ (Table 5). Replacing In with Sn does not lead to significant changes in the values of sound velocities. An increase in the concentration of simple metals leads to a decrease in [100]v_l and an increase in the transverse modes also (Table 6).

TABLE 5. The anisotropic sound velocities (in m/s) in alloys InY$_3$Ti$_{11}$

Alloy	[100]v_l	[010]v_{t1}	[001]v_{t2}	[110]v_l	[1-10]v_{t1}	[001]v_{t2}	[111]v_l	[11-2]v_{t1}	[1-10]v_{t2}
InTi$_3$Ti$_{11}$	4760	2510	2510	5171	1490	2510	5300	1892	1892
InV$_3$Ti$_{11}$	5519	2594	2594	5554	2518	2594	5566	2543	2543
InCr$_3$Ti$_{11}$	5752	2218	2218	5476	2832	2218	5381	2643	2643
InZr$_3$Ti$_{11}$	4521	2418	2418	4919	1446	2418	5044	1828	1828
InNb$_3$Ti$_{11}$	5000	2248	2248	5107	1990	2248	5143	2080	2080
InMo$_3$Ti$_{11}$	5134	1931	1931	5057	2124	1931	5031	2062	2062
InHf$_3$Ti$_{11}$	3736	2169	2169	4278	600	2169	4444	1344	1344
InTa$_3$Ti$_{11}$	4415	2416	2416	4721	1744	2416	4819	1994	1994
InW$_3$Ti$_{11}$	4668	2162	2162	4749	1978	2162	4775	2041	2041

TABLE 6. The anisotropic sound velocities (in m/s) in alloys XIn$_3$Ti$_{11}$

Alloy	[100]v_l	[010]v_{t1}	[001]v_{t2}	[110]v_l	[1-10]v_{t1}	[001]v_{t2}	[111]v_l	[11-2]v_{t1}	[1-10]v_{t2}
TiIn$_3$Ti$_{11}$	4625	3315	3315	5511	1419	3315	5776	2238	2238
VIn$_3$Ti$_{11}$	4679	3407	3407	5608	1433	3407	5885	2288	2288
CrIn$_3$Ti$_{11}$	4502	3020	3020	5310	1092	3020	5553	1958	1958
ZrIn$_3$Ti$_{11}$	4615	3252	3252	5391	1677	3252	5626	2324	2324
NbIn$_3$Ti$_{11}$	4625	3231	3231	5424	1555	3231	5665	2257	2257
MoIn$_3$Ti$_{11}$	4521	2990	2990	5249	1353	2990	5470	2050	2050
HfIn$_3$Ti$_{11}$	4393	3162	3162	5165	1617	3162	5398	2253	2253
TaIn$_3$Ti$_{11}$	4420	3174	3174	5218	1544	3174	5458	2225	2225
WIn$_3$Ti$_{11}$	4343	2918	2918	5059	1333	2918	5277	2005	2005

Thermal conductivity (k_{ph}) reflects atomic interaction within crystal at a certain temperature. The calculation of the lattice thermal conductivity of the alloys was carried out within the Slack's model [41] using the empirical formula:

$$k_{ph} = \frac{AV_0 M_a \Theta_D^3}{T\gamma_a^2 n^{2/3}}, \qquad (12)$$

where V_0 is the volume per atom, M_a is the average atomic mass per atom, T is the temperature, n is the number of atoms in the computational cell, A is a coefficient depending on the acoustic Grüneisen parameter γ_a. The coefficient A can be calculated as follows:

$$A = \frac{2.43 \cdot 10^{-8}}{1 - 0.514/\gamma_a + 0.228/\gamma_a^2}. \qquad (13)$$

Figure 3 shows the temperature dependences of k_{ph}. The highest values of the thermal conductivity in each series of alloys, for example, calculated for a temperature of 300 K are 1.64 W/(m·K) for InV$_3$Ti$_{11}$, 2.18 W/(m·K) for SnV$_3$Ti$_{11}$, 2.15 W/(m·K) for HfIn$_3$Ti$_{11}$, and 3.15 W/(m·K) for HfSn$_3$Ti$_{11}$. The lowest values of k_{ph} at the same temperature are: 0.18 W/(m·K) for InHf$_3$Ti$_{11}$, 0.17 W/(m·K) for SnHf$_3$Ti$_{11}$, 0.71 W/(m·K) for CrIn$_3$Ti$_{11}$, and 0.37 W/(m·K) for WSn$_3$Ti$_{11}$. In general, there is a correlation between the values of thermal conductivity and Debye temperature. This is especially pronounced for the alloys of the first two series, i.e. for In and Sn in the X-position. At the same time, in alloys with a large concentration of simple metals (In and Sn in the Y-position) compared to transition metals (in the X-position), this trend may be imperfect, since close values of Θ_D were obtained for several alloys. As can be seen from Fig. 3, the thermal conductivity decreases sharply with increasing temperature, and at $T > 600$ K the decrease in the thermal conductivity slows down.

The theoretical lower limit of the thermal conductivity is known as intrinsic minimum lattice thermal conductivity $k_{\min}$ of a crystal. It can be calculated using two models: Clarke's model [42, 43] and Cahill's model [44]. In the Clarke's
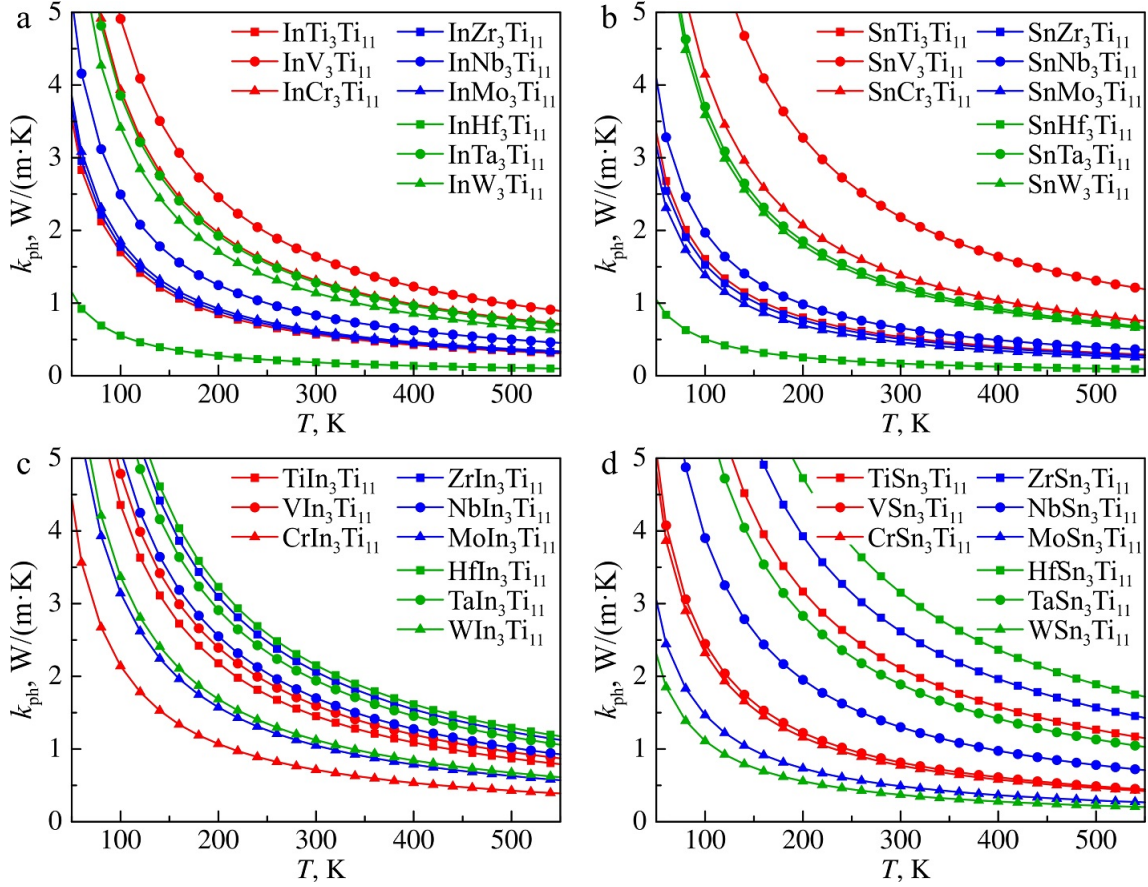
FIG. 3. Calculated lattice thermal conductivities k_{ph} in the temperature ranging from 50 to 550 K for four series of alloys: InY_3Ti_{11} (a), SnY_3Ti_{11} (b), XIn_3Ti_{11} (c), XSn_3Ti_{11} (d), where X and Y are elements of IVB–VIB groups

model,

$$k_{\min} = 0.87 k_B M_a^{-2/3} E^{1/2} \rho^{1/6}, \tag{14}$$

$$M_a = \frac{M}{mN_a}, \tag{15}$$

where M_a is the average atomic mass, M is the molar mass, and m is the total number of atoms.

In Cahill's model $k_{\min}$ is expressed as

$$k_{\min} = \frac{k_B}{2.48} n^{2/3} (v_l + 2v_t). \tag{16}$$

It is seen from Table 7 that the highest values of $k_{\min}$ in each series are observed for the InV_3Ti_{11}, SnV_3Ti_{11}, VIn_3Ti_{11}, and $ZrSn_3Ti_{11}$ alloys. The $k_{\min}$ values calculated using Clarke's model are somewhat lower than the values obtained by Cahill's model, which is due to the fact that Clarke's model does not take into account the contribution of the phonon spectrum [45]. In addition, the k_{ph} results calculated using Slack's model at high temperatures (Fig. 3) are close to those obtained using Clarke's formula. It is seen that for all alloys there is a correlation between the high $k_{\min}$ value and the Debye temperature (Table 4). In the case of VIn_3Ti_{11} and $ZrIn_3Ti_{11}$, practically the same thermal conductivity values were obtained, and the difference in the Debye temperature values is insignificant, it is approximately 4.3 K. Besides, smaller γ_a values also indicate higher thermal conductivity but this trend is imperfect with increase of s, p-element concentration.

4. Conclusion

The elastic and some thermal properties of ternary titanium alloys of the composition InY_3Ti_{11}, SnY_3Ti_{11}, XIn_3Ti_{11}, and XSn_3Ti_{11}, where X and Y are transition metals of IVB–VIB groups, are calculated using the projector augmented wave method within the density functional theory. It is shown that the values of Young's modulus for almost all alloys are lower than those of pure titanium and the Ti-6Al-4V alloy used for practical applications. The minimum values of Young's modulus (~ 37 GPa) are obtained for the alloys with Hf in the Y-position, which demonstrate a weaker interaction of the X and Y atoms with the titanium atoms located on the second coordination sphere. This trend (low C_{11} corresponds to

TABLE 7. Calculated values of $k_{\min}$ (in W/(m·K)) for series of alloys $In(Sn)Y_3Ti_{11}$ and $XIn(Sn)_3Ti_{11}$

Alloy	$k_{\min}^{\text{Clarke}}$	$k_{\min}^{\text{Cahill}}$	Alloys	$k_{\min}^{\text{Clarke}}$	$k_{\min}^{\text{Cahill}}$	Alloy	$k_{\min}^{\text{Clarke}}$	$k_{\min}^{\text{Cahill}}$	Alloys	$k_{\min}^{\text{Clarke}}$	$k_{\min}^{\text{Cahill}}$
$InTi_3Ti_{11}$	0.60	0.74	$SnTi_3Ti_{11}$	0.60	0.74	$TiIn_3Ti_{11}$	0.67	0.78	$TiSn_3Ti_{11}$	0.69	0.80
InV_3Ti_{11}	**0.77**	**0.90**	SnV_3Ti_{11}	**0.79**	**0.92**	VIn_3Ti_{11}	**0.69**	**0.80**	VSn_3Ti_{11}	0.61	0.75
$InCr_3Ti_{11}$	0.76	0.90	$SnCr_3Ti_{11}$	0.74	0.89	$CrIn_3Ti_{11}$	0.59	0.72	$CrSn_3Ti_{11}$	0.60	0.73
$InZr_3Ti_{11}$	0.55	0.68	$SnZr_3Ti_{11}$	0.54	0.67	$ZrIn_3Ti_{11}$	0.69	0.79	$ZrSn_3Ti_{11}$	**0.72**	**0.82**
$InNb_3Ti_{11}$	0.62	0.76	$SnNb_3Ti_{11}$	0.59	0.73	$NbIn_3Ti_{11}$	0.68	0.79	$NbSn_3Ti_{11}$	0.65	0.77
$InMo_3Ti_{11}$	0.60	0.75	$SnMo_3Ti_{11}$	0.57	0.73	$MoIn_3Ti_{11}$	0.62	0.74	$MoSn_3Ti_{11}$	0.54	0.68
$InHf_3Ti_{11}$	0.39	0.53	$SnHf_3Ti_{11}$	0.39	0.53	$HfIn_3Ti_{11}$	0.67	0.76	$HfSn_3Ti_{11}$	0.72	0.81
$InTa_3Ti_{11}$	0.61	0.71	$SnTa_3Ti_{11}$	0.61	0.71	$TaIn_3Ti_{11}$	0.67	0.77	$TaSn_3Ti_{11}$	0.67	0.78
InW_3Ti_{11}	0.62	0.73	SnW_3Ti_{11}	0.61	0.73	WIn_3Ti_{11}	0.61	0.72	WSn_3Ti_{11}	0.49	0.63

a lower value of E) becomes less perfect with an increase in the concentration of the s, p-element. The trends in the change of the shear modulus and Young's modulus in the studied alloys with an increase in the number of d-electrons of the transition metal are similar, and their behavior demonstrates a non-monotonic character. The decrease of Young's modulus in the series of alloys with In and Sn in the Y-position with an increase in the number of d-electrons of the X-element is also observed.

The studied ternary alloys mainly have a ductile fracture character according to three empirical criteria, although with an increase in the concentration of s, p-elements, the ionic contribution increases, which leads to an increase in the brittleness and microhardness of the alloys. In addition, with an increase in the concentration of simple metals, the brittleness index also increases and the maximum values of 3.93 and 4.58 $\mu m^{-1/2}$ were obtained for alloys with Hf in the X-position. That is, in alloys with a lower hafnium concentration, there is a decrease in the fracture (damage) resistance.

The Debye temperature was estimated for all considered ternary alloys and it was found that its lower values correlate with low values of the Young's modulus. The calculation of thermal conductivity showed that it correlates with the Debye temperature (large Θ_D corresponds to alloys with higher thermal conductivity and larger Young's moduli). In alloys with simple metals in the Y-position, i.e. with their high concentration, this trend can be imperfect. In general, the influence of s, p-elements on elastic and thermal characteristics is less pronounced compared to transition metals, regardless of the X or Y position they occupy, and reflects mainly the size effect, whereas the influence of transition metals depends significantly on the number of d-electrons of alloying elements.

References

[1] Gunther V.E., Kotenko V.V., Mirgazizov M.Z., Polenichkin V.K., Vityugov I.A., Itin V.I., Ziganshin R.V., Temerhanov F.T. *Shape memory alloys in medicine*. TSU Publ., Tomsk, 1986, 208 p. (in Russian)

[2] Long M., Rack H.J. Titanium alloys in total joint replacement – a materials science perspective. *Biomater.*, 1998, **19**, P. 1622–1639.

[3] Niinomi M. Recent research and development in titanium alloys for biomedical applications and healthcare goods. *Sci. Technol. Adv. Mater.*, 2003, **4**, P. 445–454.

[4] Niinomi M. Mechanical biocompatibilities of titanium alloys for biomedical applications. *J. Mech. Behav. Biomed. Mater.*, 2008, **1**, P. 30–42.

[5] Zhang L.C., Chen L.Y. A review on biomedical titanium alloys: recent progress and prospect. *Adv. Eng. Mater.*, 2019, **21**, 1801215.

[6] Mohammed M.T., Khan Z.A., Siddiquee A.N. Beta titanium alloys: the lowest elastic modulus for biomedical applications: a review. *Int. J. Mater. Metall. Eng.*, 2014, **8** (8), P. 822–827.

[7] Yu Z. *Titanium alloys for biomedical development and applications. Design, microstructure, properties, and application*. Elsevier, Amsterdam, 2022, 232 p.

[8] Hao C.P., Wang Q., Ma R.T., Wang Y.M., Qiang J.B., Dong C. Cluster-plus-glue-atom model in bcc solid solution alloys. *Acta Phys. Sin.*, 2011, **60** (11), 116101.

[9] Yan X., Cao W., Li H. Novel biomedical Ti-based alloys with low Young's modulus: a first-principles study. *J. Mater. Eng. Perform.*, 2024, **33**, P. 6835–6842.

[10] Kasparyan S.O., Bakulin A.V., Kulkova S.E. Mechanical properties of ternary XY_3Ti_{11} alloys. *Izvestiya vuzov. Fizika*, 2024, **67**, P. 77–85. (in Russian)

[11] Bai H., Duan Y., Qi H., Peng M., Li M., Zheng S. Anisotropic elastic and thermal properties and damage tolerance of CrH: A first-principles calculation. *Vacuum*, 2024, **222**, 112962.

[12] Sun Y., Yang A., Duan Y., Shen L., Peng M., Qi H. Electronic, elastic, and thermal properties, fracture toughness, and damage tolerance of TM_5Si_3B (TM = V and Nb) MAB phases. *Int. J. Refract. Met. Hard Mater.*, 2022, **103**, 105781.

[13] Blöchl P.E. Projector augmented-wave method. *Phys. Rev. B*, 1994, **50** (24), P. 17953–17979.

[14] Kresse G., Joubert D. From ultrasoft pseudopotentials to the projector augmented-wave method. *Phys. Rev. B*, 1999, **59** (3), P. 1758–1775.

[15] Kresse G., Hafner J. Ab initio molecular-dynamics simulation of the liquid-metal–amorphous-semiconductor transition in germanium. *Phys. Rev. B*, 1994, **49** (20), P. 14251–14269.

[16] Kresse G., Furthmüller J. Efficiency of ab-initio total energy calculations for metals and semiconductors using a plane-wave basis set. *Comput. Mater. Sci.*, 1996, **6**, P. 15–50.

[17] Perdew J.P., Burke K., Ernzerhof M. Generalized gradient approximation made simple. *Phys. Rev. Lett.*, 1996, **77** (18), P. 3865–3868.

[18] Monkhorst H.J., Pack J.D. Special points for Brillouin-zone integrations. *Phys. Rev. B*, 1976, **13** (12), P. 5188–5192.

[19] Born M., Huang K. *Dynamic theory of crystal lattices*. Oxford University Press, London, 1954, 420 p.

[20] Hill R. The elastic behaviour of a crystalline aggregate. *Proc. Phys. Soc. London, Sect. A*, 1952, **65**, P. 349–354.

[21] Voigt W. Bestimmung der Elastizitätskonstanten von Eisenglanz. *Ann. Phys.*, 1907, **327** (1), P. 129–140.

[22] Reuss A. Berechnung der Fließgrenze von Mischkristallen auf Grund der Plastizitätsbedingung für Einkristalle. *Z. Angew. Math. Mech.*, 1929, **9** (1), P. 49–58.

[23] Ledbetter H., Ogi H., Kai S., Kim S., Hirao M. Elastic constants of body-centered-cubic titanium monocrystals. *J. Appl. Phys.*, 2004, **95** (9), P. 4642–4644.

[24] Zhang Z., Li B., Chen L., Qin F., Hou Y. Measurement of elastic constants of additive manufactured Ti-6Al-4V by non-contact multi-mode laser ultrasonic system. *J. Mater. Eng. Perform.*, 2022, **31**, P. 7328–7336.

[25] Pugh S.F. Relations between the elastic moduli and the plastic properties of polycrystalline pure metals. *The London, Edinburgh, and Dublin Philosophical Magazine and Journal of Science*, 1954, **45** (367), P. 823–843.

[26] Tian Y., Xu B., Zhao Z. Microscopic theory of hardness and design of novel superhard crystals. *Int. J. Refract. Met. Hard Mater.*, 2012, **33**, P. 93–106.

[27] Bakulin A.V., Kulkova S.E. Effect of impurities on the formation energy of point defects in the γ-TiAl alloy. *J. Exp. Theor. Phys.*, 2018, **127** (6), P. 1046–1058.

[28] Niu H., Niu S., Oganov A.R. Simple and accurate model of fracture toughness of solids. *J. Appl. Phys.*, 2019, **125**, 065105.

[29] Gong X., Sun C.C. A new tablet brittleness index. *Eur. J. Pharm. Biopharm.*, 2015, **93**, P. 260–266.

[30] Munro R.G., Freiman S.W., Baker T.L. *Fracture toughness data for brittle materials*. NIST Publ., Gaithersburg, 1998, 153 p.

[31] Moruzzi V.L., Janak J.F., Schwarz K. Calculated thermal properties of metals. *Phys. Rev. B*, 1988, **37** (2), P. 790–799.

[32] Liu X., Fu J. First principle study on electronic structure, elastic properties and Debye temperature of pure and doped $KCaF_3$. *Vacuum*, 2020, **178**, 109504.

[33] Music D., Houben A., Dronskowski R., Schneider J.M. Ab initio study of ductility in M_2AlC (M = Ti, V, Cr). *Phys. Rev. B*, 2007, **75**, 174102.

[34] Anderson O.L. A simplified method for calculating the Debye temperature from elastic constants. *J. Phys. Chem. Solids*, 1963, **24**, P. 909–917.

[35] Anderson O.L. The high-temperature acoustic Grüneisen parameter in the earth's interior. *Physics of the Earth and Planetary Interiors*, 1979, **18**, P. 221–231.

[36] Vitos L. *Computational quantum mechanics for materials engineers: the EMTO method and applications*. Springer, London, 2007, 236 p.

[37] Kerley G.I. *Equations of state for titanium and $Ti_6A_{14}V$ alloy*. Sandia National Lab., Oak Ridge, 2003, 35 p.

[38] Leont'ev K.L. On the relationship between elastic and thermal properties of substances. *Sov. Phys. Acoust.*, 1981, **27**, P. 309–316.

[39] Belomestnykh V.N. The acoustical Grüneisen constants of solids. *Tech. Phys. Lett.*, 2004, **30** (2), P. 91–93.

[40] Kittel C. *Introduction to solid state physics*, 8th ed. John Wiley & Sons, Hoboken, 2005, 681 p.

[41] Shindé S.L., Goela J.S. *High thermal conductivity materials*. Springer, New York, 2006, 271 p.

[42] Hoel H., Nyberg H. An extension of Clarke's model with stochastic amplitude flip processes. *IEEE Trans. Commun.*, 2014, **62** (7), P. 2378–2389.

[43] Clarke D.R., Levi C.G. Materials design for the next generation thermal barrier coatings. *Annu. Rev. Mater. Res.*, 2003, **33**, P. 383–417.

[44] Cahill D.G., Watson S.K., Pohl R.O. Lower limit to the thermal conductivity of disordered crystals. *Phys. Rev. B*, 1992, **46** (10), P. 6131–6140.

[45] Duan Y.H., Sun Y., Lu L. Thermodynamic properties and thermal conductivities of $TiAl_3$-type intermetallics in Al–Pt–Ti system. *Comput. Mater. Sci.*, 2013, **68**, P. 229–233.

Information about the authors:

Sergey O. Kasparyan – Institute of Strength Physics and Materials Science of the Siberian Branch of the Russian Academy of Sciences, Akademicheskii, 2/4, Tomsk, 634055, Russia; National Research Tomsk State University, Lenina, 36, Tomsk, 634050, Russia; ORCID 0000-0002-0234-884X; ks-ftf-isopams@mail.ru

Adil E. Ordabaev – National Research Tomsk State University, Lenina, 36, Tomsk, 634050, Russia; ORCID 0009-0008-4124-450X; adil.ordabaev04@gmail.com

Alexander V. Bakulin – Institute of Strength Physics and Materials Science of the Siberian Branch of the Russian Academy of Sciences, Akademicheskii, 2/4, Tomsk, 634055, Russia; ORCID 0000-0001-5099-3942; bakulin@ispms.ru

Svetlana E. Kulkova – Institute of Strength Physics and Materials Science of the Siberian Branch of the Russian Academy of Sciences, Akademicheskii, 2/4, Tomsk, 634055, Russia; ORCID 0000-0002-7155-3492; kulkova@ispms.ru

Conflict of interest: the authors declare no conflict of interest.